ISSUE: September 2022

Inverter With Modified PLL Control Transitions Seamlessly Between On- And Off-Grid Operation

by Basil Issac, Eram Power Electronics, Bangalore, India

The phase, amplitude and frequency of the utility grid are critical information for the operation of grid-connected inverters. In such applications, an accurate and fast detection of the phase angle of the utility voltage is essential to assure correct generation of the reference signals for synchronizing operation of the inverters with the grid. Another key element in these applications is the phase-locked loop (PLL) structure, which is a feedback control system that automatically adjusts the phase of a locally generated signal to match the phase of an input signal.

In a grid-connected system, the purpose of the PLL is to synchronize the inverter voltage phase angle with the angle of the grid voltage, in order to obtain zero phase shift and frequency difference between the grid voltage and the inverter. In this article, a PLL-based control technique for a grid-connected inverter is introduced and simulated using MATLAB software.

The technique presented here uses an internal droop controller with additional voltage feedback and an external PLL configuration to synchronize the inverter with the grid. The uniqueness of this PLL control technique lies in how the PLL is configured. The advantage of this technique is that it ensures seamless transfer of the inverter between on-grid and off-grid operation. The purpose of the droop control is to ensure proper active and reactive power sharing between inverters by maintaining constant voltage and frequency, while reducing the voltage distortion to a considerable extent.

The operations sequence for this PLL control technique has been divided into three tasks to explain and demonstrate how it functions. In task 1, we'll see how a PLL performs the basic operations of voltage droop and frequency drop detection, which are necessary to synchronize an inverter with the grid.

In task 2, the PLL is modified to provide more-robust droop control. We'll then simulate the use of this technique in syncing an inverter to the grid, and then observe the inverter's performance as it shares a load with the grid, and as the full load is shifted to the inverter with the inverter in island mode.

Task 2 tests the PLL control technique with a dc power source powering the inverter. However, in task 3, the same operations will be simulated again with a fuel cell providing power to the inverter. This illustrates the usefulness of the proposed technique in power systems with distributed energy sources.

Task 1: Implementing Voltage Droop And Frequency Drop Detection

The phase synchronization is important in grid inverters, otherwise a tiny difference in frequency between the grid ac waveform and the inverter ac waveform could lead to a very large voltage difference! It is crucial to synchronize two ac voltage sources before connecting them together. Here, the ability of a PLL to detect voltage droop and frequency reduction are demonstrated and we'll see the general response time of a PLL in the usual configuration.

A sinusoidal measurement PLL, the block shown in Fig. 1 implements a PLL to estimate the characteristics of a sinusoid. The block outputs the frequency (Hz), angle (rad), and magnitude for a single-phase input signal.

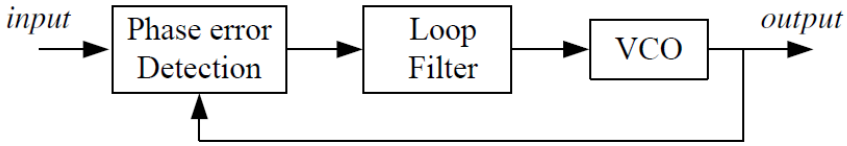

Fig. 1. Fundamentals of a PLL.

In this PLL, a phase (error) detection (PD) unit measures the phase difference between the input signal and the reproduced output signal and a loop filter (LF) extracts the dc component obtained from the phase error. A voltage-controlled oscillator (VCO), which is often a PI controller, then generates the frequency of the output signal.

If the frequency of the output signal is locked with the input frequency, then the phase difference between the input and output signals, i.e. the output of the PD, is eventually driven to zero. As a result, the phase of the output signal is *locked* with that of the input signal.

Fig. 2 shows the implementation of task 1. Here, source-1 implements a 60-Hz,169.7-V peak ac voltage, while source 2 generates a signal with the same frequency but the voltage drops by 20% and source 3 generates a signal of the same amplitude as source 1 but the frequency drops from 60 Hz to 59 Hz. In this circuit configuration, all three sources represent the grid waveform and the simulations that follow demonstrate how the PLL tracks the voltage and frequency changes.

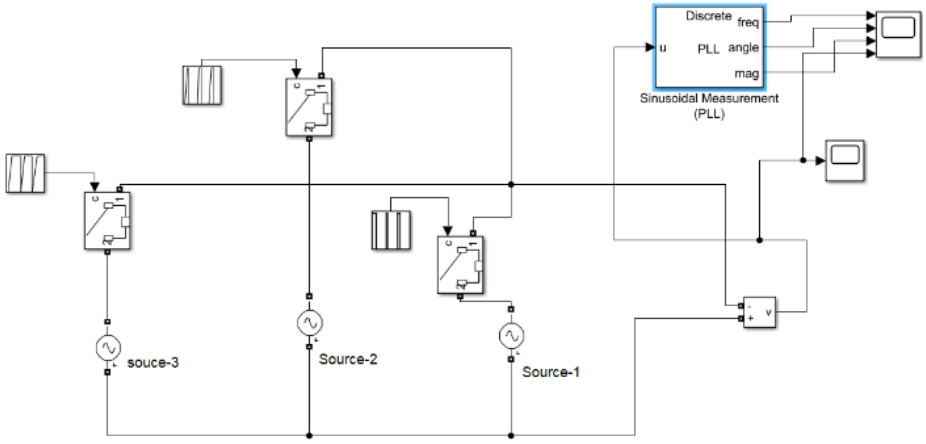

Fig. 2. Set up for single-phase PLL implementation for task 1.

Fig. 3 shows the source 1 60-Hz frequency represented as a dc voltage (top waveform), the PLL angle output (middle waveform) and the grid voltage (bottom waveform). By comparing the middle and bottom waveforms in Fig. 3, it can be seen that the PLL phase angle is synchronized with the grid voltage.

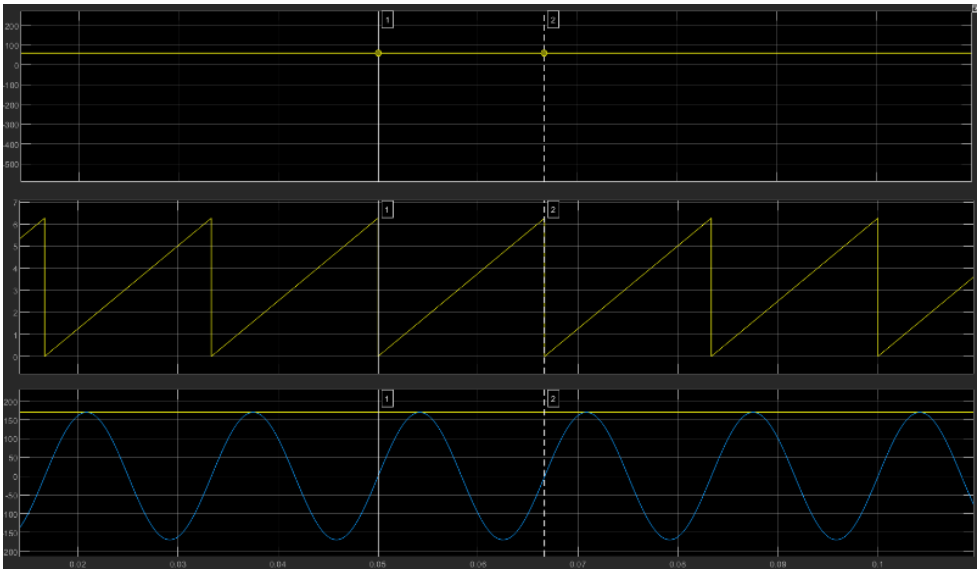

Fig. 3. Waveforms for source 1 frequency (top trace), PLL output angle (middle trace) and grid voltage (RMS and sine representation, bottom blue trace).

Fig. 4 simulates the condition represented by source 2 where the grid voltage (bottom waveform) drops by 20%. In this case, the PLL output responds within ~5 cycles to bring down the magnitude (refer to the yellow line in the bottom waveform of Fig. 3) of the voltage, and it achieves a constant value in 15 cycles of the fundamental voltage. Ideally, we would like this constant value to be reached more quickly. Note that the PLL frequency and the source voltage frequency remain the same.

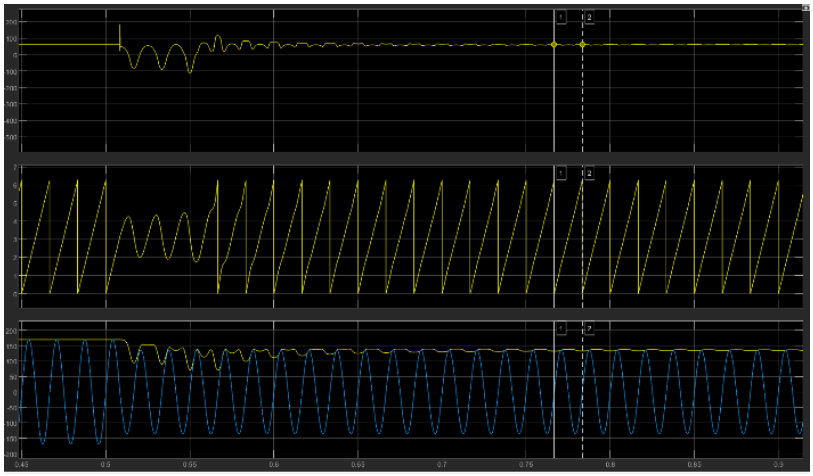

Fig. 4. Response of the PLL when source voltage (source 2) drops by 20%.

Fig. 5 simulates the condition in source 3 where the frequency drops from 60 to 59 Hz. Here, the frequency drop has been detected in the top waveform of Fig. 5. The PLL output (middle waveform) tracks the frequency change dynamically and corrects the angle based on the new frequency, 59 Hz. A comparison of the PLL angle output versus the grid voltage with the new frequency has been shown in the middle and bottom waveforms of Fig. 5. It has been shown that the PLL phase and the grid voltage zero crossing track without any phase delay.

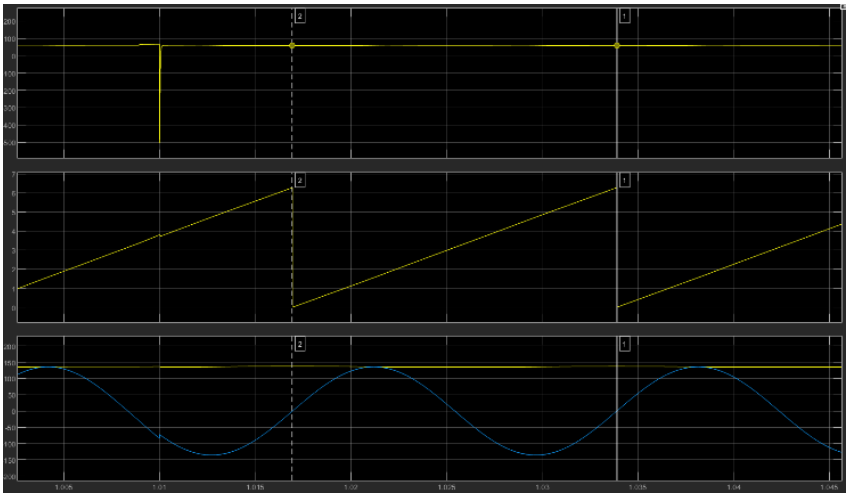

Fig. 5. Response of the PLL when the frequency drops from 60 Hz to 59 Hz (source 3).

It has been seen from the simulation that a PLL is a control system that generates an output signal whose phase is related to the phase of an input signal. Phase-locked loops are widely used for synchronization purposes. In PLL applications it is frequently required to know when the loop is out of lock.

Task 2: Implementation Of More-Robust Droop Control

Before exploring how the performance of a PLL can be improved, we need to review how a conventional droop controller operates. Fig. 6 shows graphically how a conventional droop controller works in terms of tracking a differences in waveform amplitude and phase.

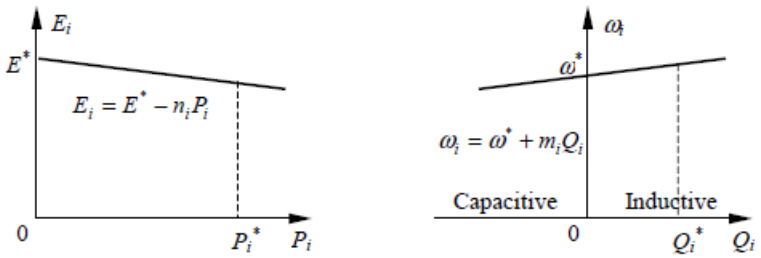

Fig. 6. Operation of a conventional droop controller.

The key equations here are

$E_i = E* - n_i P_i$

$w_i = w* + m_i Q_i$

where P represents real power or active power, Q is reactive power, and n_i and m_i are droop coefficients. In addition P and Q are defined as

P = (Evo/Zo*cos δ −Vo^2/Zo) cosq + Evo/Zo*sin δ *sinq

Q= (Evo/Zo*cos δ −Vo^2/Zo) sinq - Evo/Zo*sin δ *cosq

For a resistive impedance: q = 0°, then and when δ is small,

$P = (Evo/Zo)- (Vo^2/Zo)$, $Q= -Evo/Zo* \delta$

With roughly decoupled control

$P \sim E,\ Q \sim -\delta$

$E_i = E_* - n_i P_i,\ \omega_i = \omega_* + m_i Q_i$

There are a few drawbacks to this control technique due to its droop characteristics. It is almost impossible in practice to maintain $E_1 = E_2 = \cdots = E_n$ because there are always numerical computational errors, disturbances and noise. Therefore, the conventional droop control is *not* robust! A mechanism is needed to guarantee that accurate proportional load sharing can be achieved when these uncertain factors exist.

In this section, we describe the implementation of a robust droop control technique that synchronizes an inverter with the grid voltage to achieve the seamless transfer of the load between islanded operation and grid operation. This robust droop controller is an advanced version of the conventional droop controller where an integral term is added for the voltage loop. An improved droop controller achieves accurate proportional load sharing. The output voltage droop $E_* - Vo$ is added to dE_i via an amplifier K_e to make sure that the output voltage remains within a certain required range.

In the steady state, the input to the integrator should be 0. Hence,

$$n_i P_i = K_e(E_* - V_o) = \text{constant}$$

if K_e is chosen the same. This guarantees accurate real power sharing without having the same E_i. This is more natural than the case with the conventional droop controller. The accuracy of real power sharing no longer depends on the inverter output impedances and is also immune to numerical computational errors and disturbances.

The droop coefficients n_i and m_i are calculated based on the voltage ratio defined by 5% and the frequency boost ratio of 1%.

Therefore,

$$n_i\ P_{i*}/K_e E_* = 5\%$$

and the frequency boost ratio

$$m_i\ Q_{i*}/\omega_* = 1\%$$

at the rated reactive power Q_* and real power P_* The robust droop control algorithm is shown in Fig. 7.

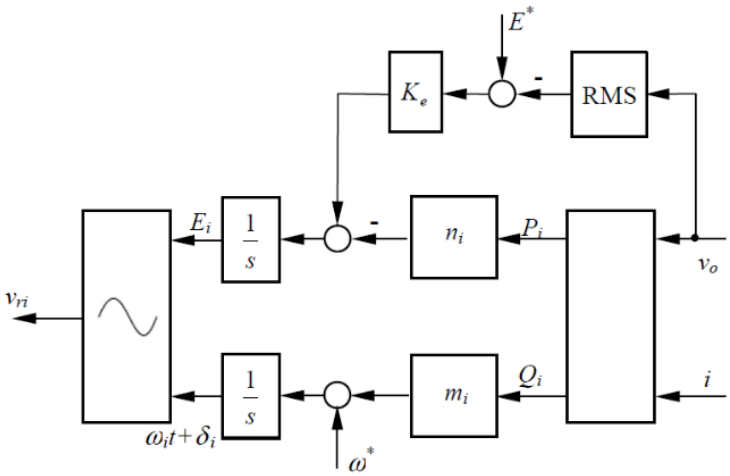

Fig. 7. Robust droop control R inverter.

Fig. 8 shows the operational sequence of task 2, where the top waveform in Fig. 8 shows the inverter voltage building up within 0.5 sec to its required 120-V rms output. A breaker CB1 is turned on at 1 sec, followed by turn-on of breaker CB2 at 1.2 sec. The breaker CB1 is then turned off at 2 sec such that the complete load is transferred to the inverter.

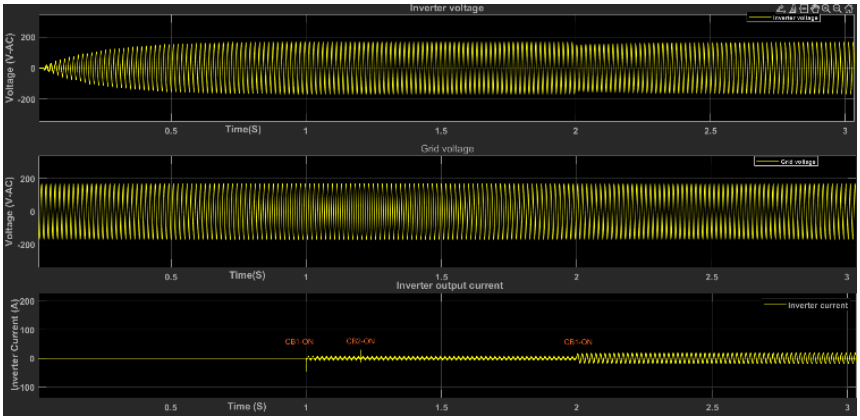

Fig. 8. Inverter and grid operation sequence. After the inverter output stabilizes and syncs with the grid, the load is connected to the inverter and then briefly shared with the grid. Finally, the grid is disconnected from the load.

Fig. 9 shows an enlarged view of operation when CB1 turns on, where the grid voltage (blue waveform) is in sync with the inverter voltage (yellow). After the breaker CB1 is on, the inverter voltage and the grid voltage are in complete synchronization. At the time of CB1 turn-on, the current overshoot measured is ~35 A, though this event is not captured in Fig. 9.

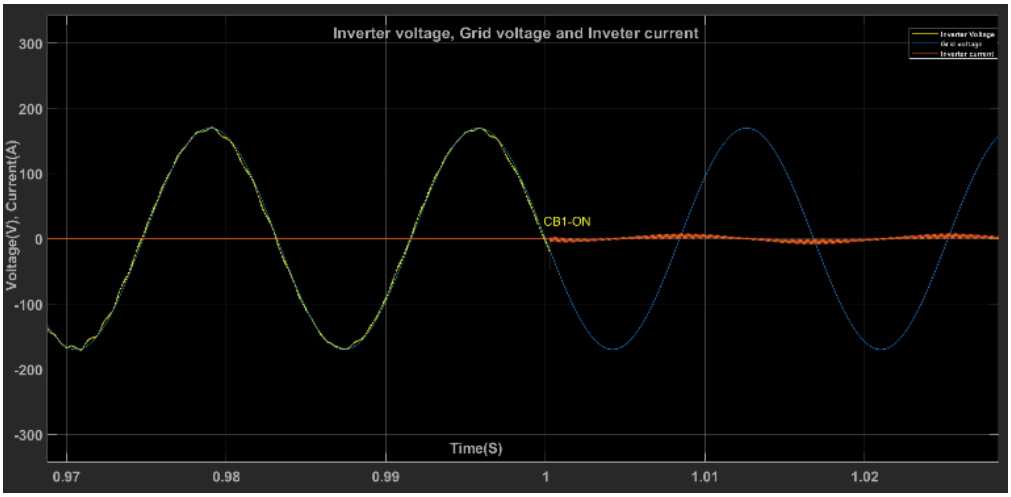

Fig. 9. Breaker CB1 turns on. A closeup of the grid (yellow) and inverter (blue) waveforms when CB1 turns on shows the two voltage waveforms are in sync. The grid carries the full load at this time.

Fig. 10 shows operation when CB2 turns on, where the inverter output and grid voltage are also in sync. The RMS voltage measured on the inverter output is 120 Vac and the frequency of the inverter output voltage is in synchronization with the grid frequency of 59.5 Hz where the initial frequency set for the inverter was 50 Hz**.**

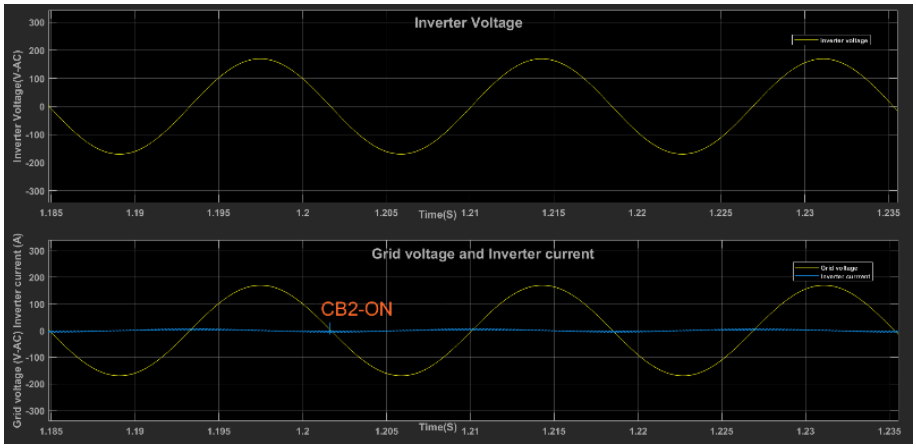

Fig. 10. CB2 turns on. The inverter and grid are sharing the load.

The turn-off operation of breaker CB1 is shown in Fig. 11, where the output load is completely transferred to the inverter. The breaker CB1 is turned off at 2 sec in the top waveform of Fig. 11, and until then the inverter output was completely in sync with the grid voltage and frequency.

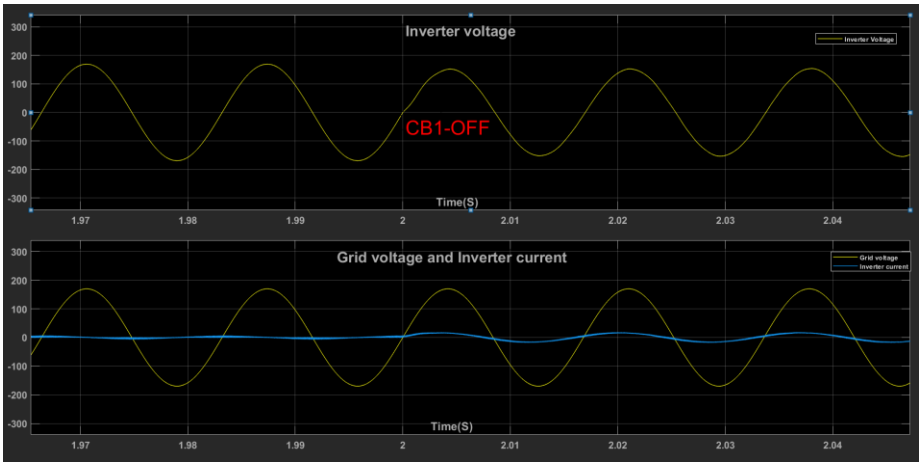

Fig. 11. CB1 off sequence. After CB1 turns off, the inverter carries the full load.

Fig. 12 shows the RMS voltage of the inverter and the regulation response for the entire operation. When CB1 is turned on, the output voltage is matched with the grid voltage (you can see this in Fig. 9 too). When CB2 is turned on, we don't see any difference in the voltage waveform as it is completely in sync with the grid voltage. When the breaker CB1 is off and the complete load is transferred to the inverter, the output voltage drops to 108 V momentary (in Fig. 12, top waveform) and then it recovers to 120 V in 1 sec of time.

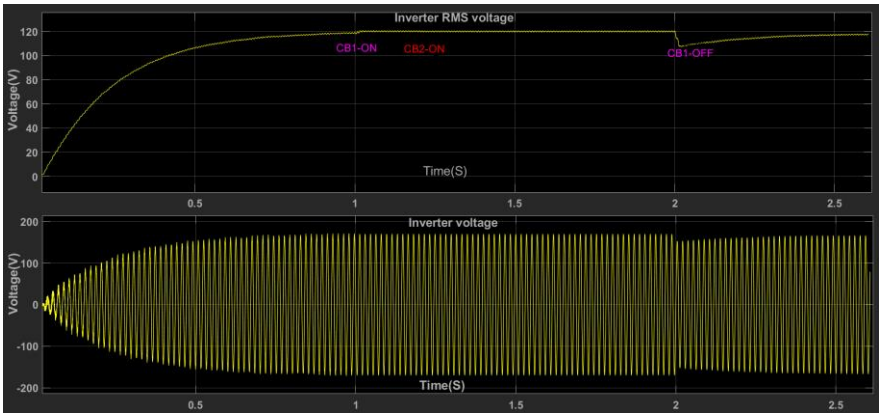

Fig. 12. The RMS voltage and waveform of the inverter are shown through the steps of powering up and syncing the inverter with the grid, applying the load to inverter and grid, and then removing the grid from the load.

Task 3: Applying More-Robust Droop Control With A Distributed Energy Source

Now, we take the concept of inverter-grid synchronization with more-robust droop control, which was simulated in task 2, and apply it to the case where the input is not a "stiff" dc supply, but rather a distributed energy resource. For example, the dc input to the inverter could be a wind turbine or a string of solar panels. The goal here is to design a distributed generation system that can be operated in the islanded mode and the grid-tied mode. We'll repeat the simulations performed in task 2.

For this task I have selected a fuel cell as the renewable energy source, implementing a generic hydrogen fuel cell model which allows the simulation for the following types of cells.

Fig. 13 shows the I-V characteristic of the fuel cell, where the voltage capability to source the current of 30 A is equal to ~55 V. I have used two such modules in parallel to get an average output voltage of ~120 V dc.

To generate 220 Vdc as the inverter input, I have implemented a boost converter as a front-end converter.

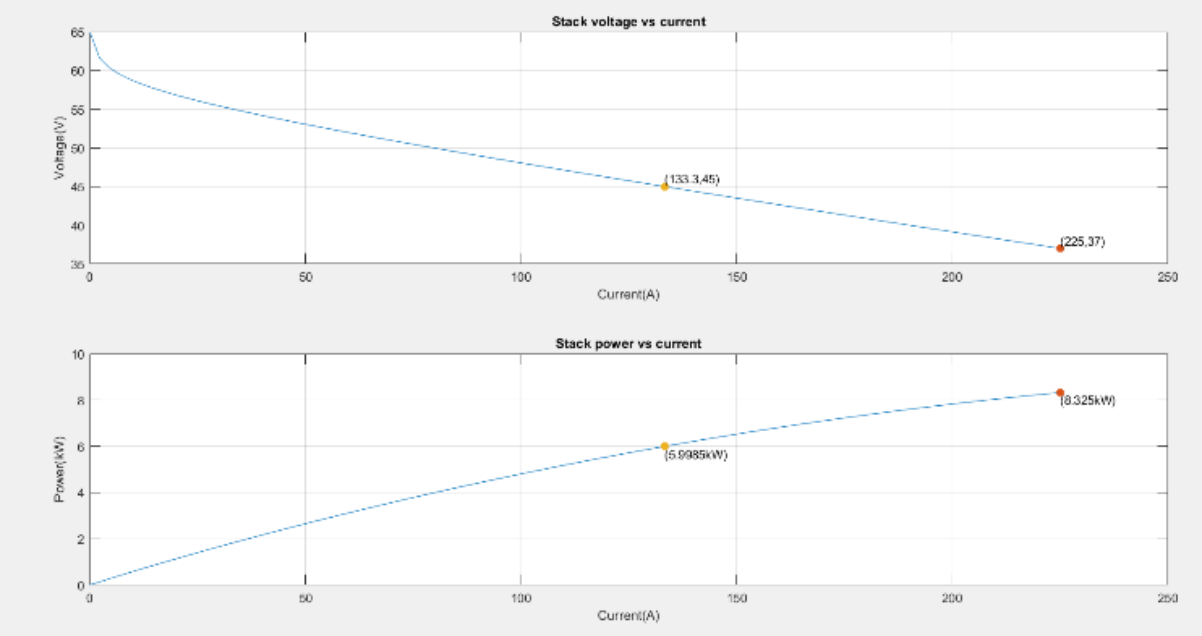

Fig. 13. I-V characteristic of the fuel cell.

Fig. 14 shows the front-end boost converter to convert the 110 V generated by fuel cells to 220 V for the inverter.

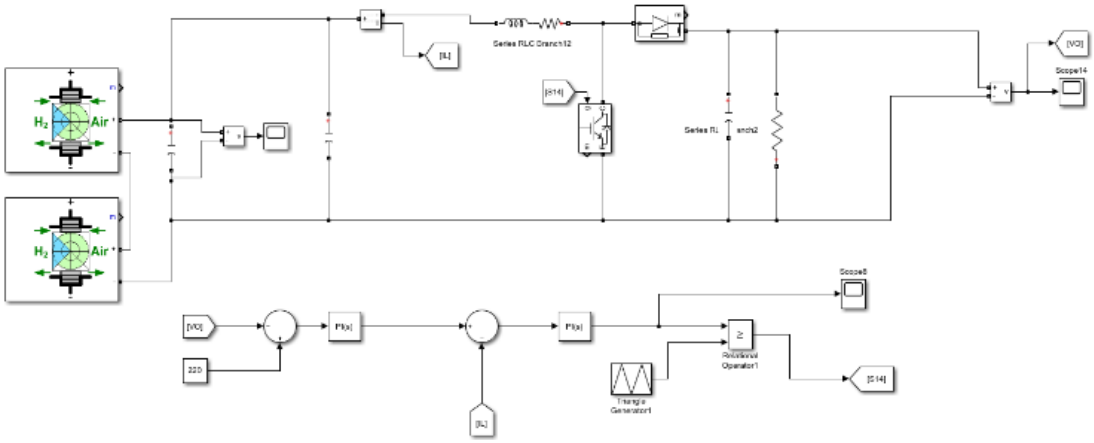

Fig. 14. Front-end fuel cell and boost converter.

Fig. 15 shows the fuel cell output voltage of ~120 V (blue waveform), where two fuel cells are connected in series to get 120 V. The fuel cells' output voltage is fed to a boost converter operating in average current control mode to boost the voltage to 220 V (yellow waveform in Fig. 15). The boost converter is implemented with an inner current loop and outer voltage loop. The outer voltage loop compares the feedback voltage against the set reference voltage of 220 V. The error is fed to a PI controller and the output of the PI controller is the inner loop current reference.

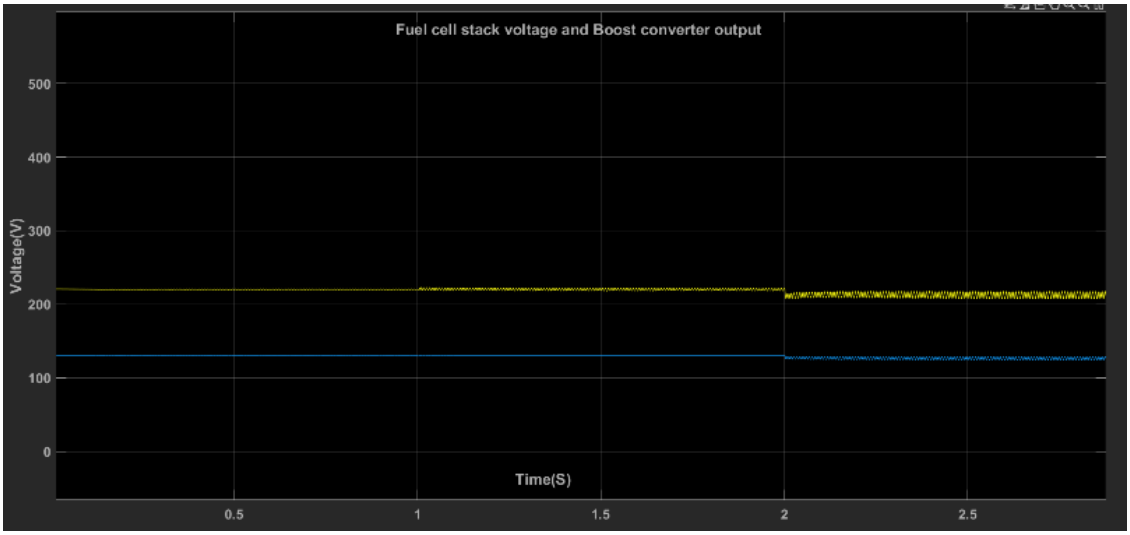

Fig. 15. Fuel cell output voltage and boost converter output voltage.

The inner current loop compares the difference between the current reference and the input current of the boost converter, and the current reference output is fed to the PI controller and to the modulator to generate the PWM.

The transfer function of the boost converter can be written

$$V_{OUT} = V_{IN}/(1\text{-}D)$$

where V_{OUT} is the output voltage, V_{IN} is the input voltage and D is the duty cycle. The transfer function clearly says that the output voltage will be greater than the input voltage, hence the boost converter generates 220-V output voltage.

Fig. 16 shows the operational sequence of task 3, where the top waveform shows the inverter voltage building up within 0.7 sec to its required 120-V rms output. A breaker CB1 is turned on at 1 sec, followed by turn-on of breaker CB2 at 1.2 sec. The breaker CB2 then turned off at 2 sec where the complete load is transferred onto the inverter. The inverter current is shown in the bottom waveform.

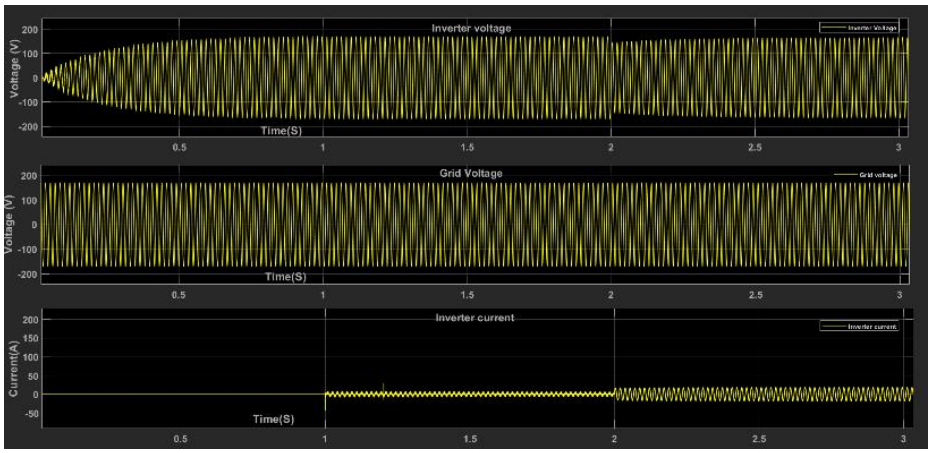

Fig. 16. Inverter and grid operation sequence where the inverter is powered from the fuel cell. All of the subsequent simulations in this section assume the use of the fuel cell.

As we did in task 2, we'll look at close-ups of the grid and inverter voltage waveforms. Fig. 17 shows the close view when CB1 turns on, where the grid voltage (blue waveform) is in sync with the inverter voltage (yellow). After the breaker CB1 is on, the inverter voltage and the grid voltage are in complete synchronization. At the time of CB1-on, the current overshoot measured is ~35 A as it was in task 2 with the dc supply. This overshoot is faintly visible in Fig. 17.

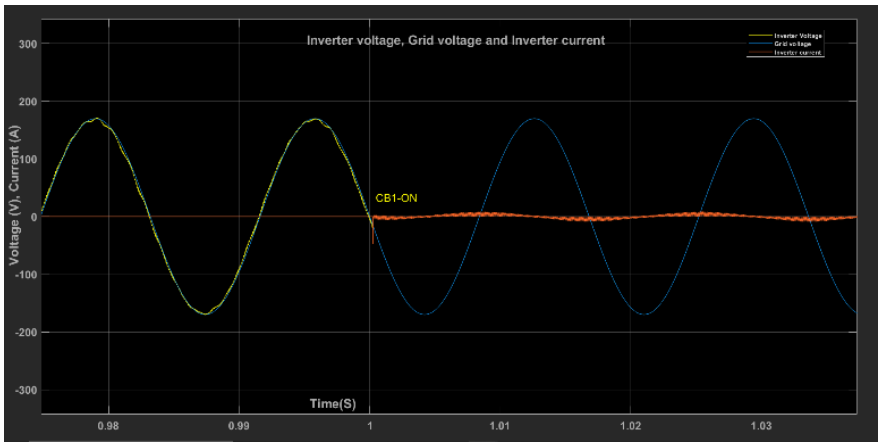

Fig. 17. Breaker CB1 turns on. Grid and inverter waveforms are present, but the load is carried by the grid. Load current is also shown.

Fig. 18 shows the waveforms when CB2 turns on where the inverter output and grid voltage are in sync. The RMS voltage measured on the inverter output is 120 Vac, the frequency of the inverter output voltage is in synchronization with the grid frequency of 59.5 Hz where the initial frequency set for the inverter was 50 Hz. The overshoot observed in the inverter current is nearly 48 A during the turn-on of breaker CB2. That can be seen in the bottom waveform of Fig. 18.

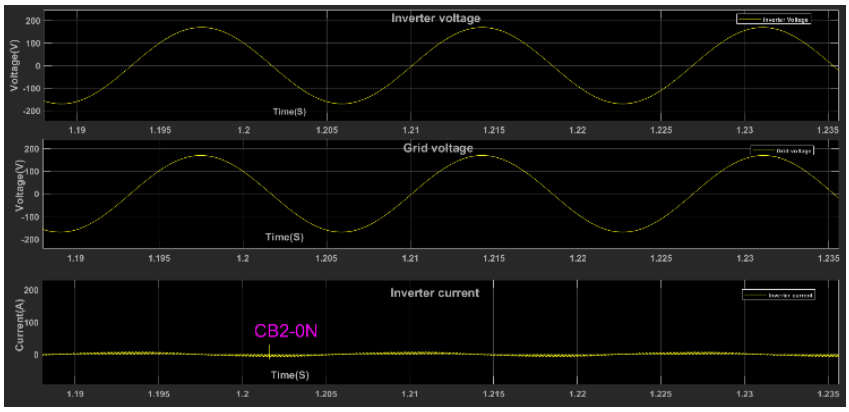

Fig. 18. CB2 turns on. The inverter and grid are in sync and sharing the load.

The turn-off operation of breaker CB1 is shown in Fig. 19, where the output load is completely transferred to the inverter. The breaker CB1 is turned off at 2 sec in the top waveform of Fig. 19. Until then the inverter output was completely in sync with the grid voltage and frequency.

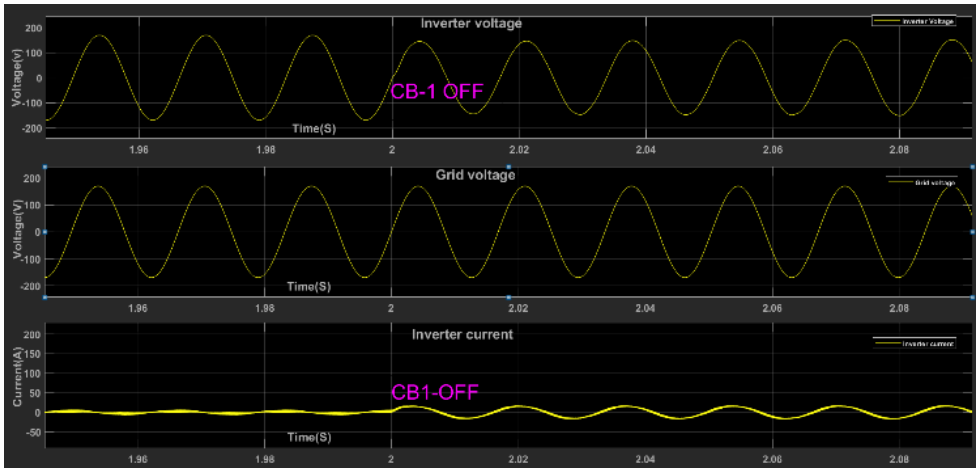

Fig. 19. CB1 off sequence. The load is transferred fully to the inverter while the inverter voltage remains in sync with the grid up until CB1 turns off.

Fig. 20 shows the RMS voltage of the inverter and the regulation response for the entire operation. When CB1 is turned on, the output voltage is matched with the grid voltage (you can see this in Fig. 9). When CB2 is turned on, we don't see any difference in the voltage waveform as it is completely in sync with the grid voltage. When the breaker CB1 goes off and the complete load is transferred to the inverter, the output voltage drops to 108 V momentarily (in Fig. 20, top waveform) and then it returns to 120 V 1 sec later.

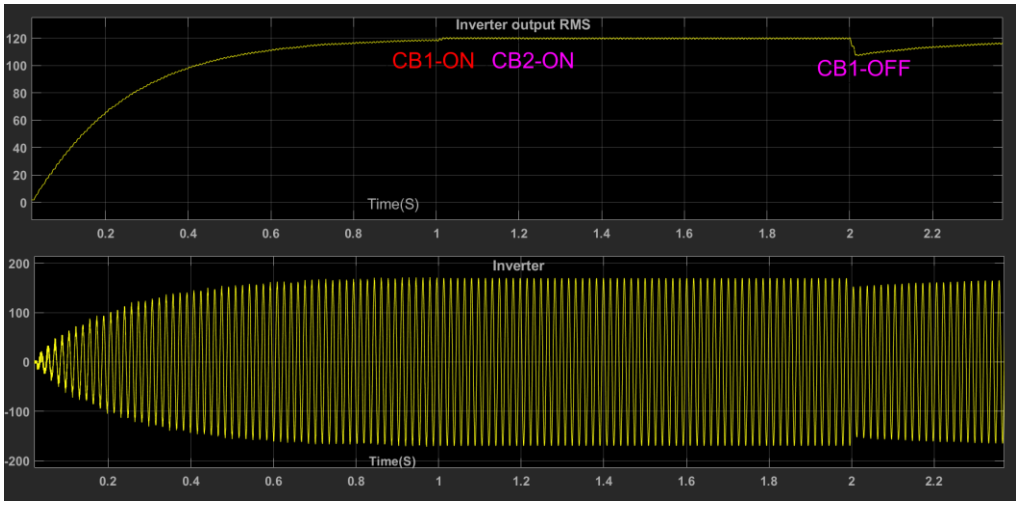

Fig. 20. The RMS voltage and output waveform of the inverter through the steps of powering up and syncing the inverter with the grid, applying the load, and then removing the grid from the load.

Consolidating The Results

The aim of this work was to design, simulate, and implement a digital PLL circuit to synchronize the generated inverter output voltage with the grid for seamless transfer of the load between the between the inverter when connected to the grid and the inverter in island operation. The PLL with more-robust droop control implements the dynamic correction of inverter frequency, phase and RMS voltage.

Fig. 21 below shows the grid frequency, grid voltage and inverter voltage. It can be seen from the figure that the inverter frequency and phase are in sync with the grid frequency and grid phase. The waveform is captured for task 3 before the breaker CB-1 is on.

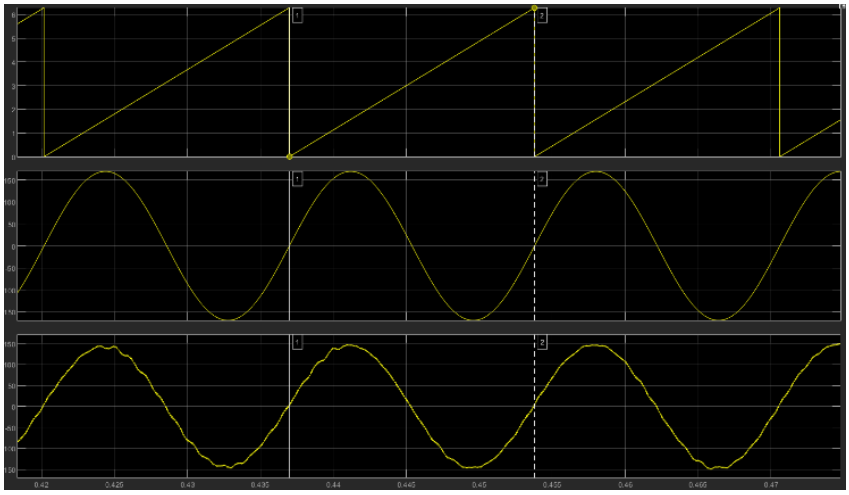

Fig. 21. Grid frequency, grid voltage and inverter voltage for task 3 before breaker CB1 turns on.

This shows how a PLL can be implemented to achieve the phase and frequency correction for a grid-connected inverter.

Conclusion

This article described a complete control strategy for a single-phase inverter operating in both grid-connected and grid-isolated (island) mode. For the synchronization of the inverter with the grid, a single-phase PLL controller was presented. The performance of the proposed PLL controller was validated through simulation under varying frequency conditions.

This article talked about the design, simulation, and the implementation of digital PLL circuit to synchronize the generated inverter output voltage with the grid for seamless transfer of the load between the grid inverter and island operation. The PLL implemented the dynamic correction of inverter frequency, phase and the RMS voltage.

The robust droop controller described here was able to share the load according to the sharing ratio and considerably outperformed the conventional droop controller in terms of sharing accuracy and voltage drop.

The grid connected system was tested under two different modes of operations, which were inverter control during grid-connected operation (CB1-on) and grid-isolated operation (CB1-off). During grid-connected operation, the inverter synchronized with the grid frequency and voltage. During isolated grid operation where CB1 was off, the inverter operated in standalone mode to maintain a constant voltage.

Reference

"Control of power inverters for the smart grid" by Qing-Chang Zhong, Proceedings of the American Control Conference, June 2014.

About The Author

Basil Issac currently serves as vice president R&D at Eram Power Electronics Bangalore, India where he takes the lead in managing the R&D and innovation center, a Saudi-based power electronics company pioneer in high-power and high-voltage battery chargers, charge controllers, frequency converters, inverters and active power factor-controlled power conditioners for ac-dc conversion.

He has 22+ years of experience in power products design and development in the field of industrial medical and aerospace. He has expertise in switch-mode power supply, power inverter/converter, and high-power current-mode inverter drives design for medical, industrial, and aerospace applications. Basil has had complete involvement in concept design, product development, processes, and successful manufacturing transfer to complete the product design execution.

Basil also has expertise in new product development in the field of power electronics for UPS, battery charger, airborne and ground vehicle applications. He holds an engineering degree in electronics and communications from Madras University and a degree in power engineering from the University of Illinois at Chicago. He can be reached at basil.issac@eramelectronics.com.

For further reading about inverter design, see the How2Power Design Guide, locate the Power Supply Function category and select "DC-AC inverters".